Low rates of bedrock outcrop erosion in the central Appalachian Mountains inferred from in situ ^{10}Be

Eric W. Portenga[1,†,§], Paul R. Bierman[2], Donna M. Rizzo[3], and Dylan H. Rood[4,#]

[1]*Department of Geology, University of Vermont, Burlington, Vermont 05405, USA*

[2]*Department of Geology and Rubenstein School of the Environment and Natural Resources, University of Vermont, Burlington, Vermont 05405, USA*

[3]*College of Engineering and Mathematical Sciences, University of Vermont, Burlington, Vermont 05405, USA*

[4]*Center for Accelerator Mass Spectrometry, Lawrence Livermore National Laboratory, Livermore, California 94550, USA,* and *Earth Research Institute, University of California, Santa Barbara, California 93106, USA*

ABSTRACT

Bedrock outcrops are common on central Appalachian Mountain ridgelines. Because these ridgelines define watersheds, the rate at which they erode influences the pace of landscape evolution. To estimate ridgeline erosion rates, we sampled 72 quartz-bearing outcrops from the Potomac and Susquehanna River Basins and measured in situ–produced ^{10}Be. Ridgeline erosion rates average 9 ± 1 m m.y.$^{-1}$ (median = 6 m m.y.$^{-1}$), similar to ^{10}Be-derived rates previously reported for the region. The range of erosion rates we calculated reflects the wide distribution of samples we collected and the likely inclusion of outcrops affected by episodic loss of thick slabs and periglacial activity. Outcrops on main ridgelines erode slower than those on mountainside spur ridges because ridgelines are less likely to be covered by soil, which reduces the production rate of ^{10}Be and increases the erosion rate of rock. Ridgeline outcrops erode slower than drainage basins in the Susquehanna and Potomac River watersheds, suggesting a landscape in disequilibrium. Erosion rates are more similar for outcrops meters to tens of meters apart than those at greater distances, yet semivariogram analysis suggests that outcrop erosion rates in the same physiographic province are similar even though they are hundreds of kilometers apart. This similarity may reflect underlying lithological and/or structural properties common to each physiographic province. Average ^{10}Be-derived outcrop erosion rates are similar to denudation rates determined by other means (sediment flux, fission-track thermochronology, [U-Th]/He dating), indicating that the pace of landscape evolution in the central Appalachian Mountains is slow, and has been since post-Triassic rifting events.

INTRODUCTION

Appalachian landscape evolution has sparked over a century of discussion. An early theory of landscape evolution suggested that after being uplifted, peneplains were dissected by the rapid downcutting of streams, which eventually achieved a graded or equilibrium profile (Davis, 1899). Davis's model persisted until Hack (1960) suggested that Appalachian landscapes were not the dissected remnants of uplifted plains, but rather resulted from the interaction of numerous driving forces including tectonics, erosion, climate, and physical properties of Earth materials. Contrary to Davis's idea that landscapes evolved directionally over time, Hack proposed that landscapes only appear to preserve landforms. In reality, these landforms are continuously being eroded and uplifted in a dynamic equilibrium, where landscapes remain similar over the large scale but individual elements come and go over time as they are dismembered by erosion.

In the Appalachian Mountains, bedrock outcrops are often observed along ridgelines that define watershed boundaries. The existence of such ridges indicates that, at least for some time in the past, the landscape within the watersheds must have eroded more quickly than the rock ridges defining the watershed boundaries. This rapid downcutting may be initiated along structural weaknesses in the rock and perhaps by the process of headward stream capture (e.g., Clark, 1989; Gunnell and Harbor, 2010; Prince et al., 2010).

Around the globe, drainage basins appear to be eroding at least as quickly as or faster than bedrock outcrops in any region where both types of samples have been analyzed (Portenga and Bierman, 2011). Measured samples collected both from drainage basins and from individual bedrock outcrops on ridgelines provide important data for understanding landscape evolution through time, allowing one to contrast the rate of ridgeline lowering with that of basins as a whole. Comparing ridgeline erosion rates to basin erosion rates has the potential to determine whether relief is changing over time—a fundamental descriptor of landscape development. However, too little is known about bedrock outcrop erosion rates in the Appalachian Mountains to make such a comparison.

Traditional methods of measuring the pace of landscape change, such as chemical mass balances, sediment budgeting, and topographic measures of cliff or slope retreat over time, are difficult to apply or are unrepresentative at both the temporal and spatial scale of outcrop erosion (Saunders and Young, 1983). In contrast, cosmogenic methods are well suited for estimating outcrop erosion rates over millennial time scales (e.g., Nishiizumi et al., 1986), and the most widely used cosmogenic nuclide for erosion rate studies is ^{10}Be measured in quartz (Portenga and Bierman, 2011).

Within the upper few meters of Earth's surface, ^{10}Be is created primarily by spallation nuclear reactions during which high-energy neutrons interact with oxygen in the mineral structure. The ^{10}Be subsequently decays radioactively ($t_{1/2}$ = 1.39 Ma; Chmeleff et al., 2010; Korschinek et al., 2010). The production of ^{10}Be

†E-mail: eporteng@uvm.edu

§Present addresses: School of Geographical and Earth Science, University of Glasgow, Glasgow G12 8QQ, Scotland, UK, and Department of Environment and Geography, Macquarie University, North Ryde, NSW 2109, Australia.

#Present address: Scottish Universities Environmental Research Centre (SUERC), East Kilbride G75 0QF, Scotland, UK.

GSA Bulletin; January/February 2013; v. 125; no. 1/2; p. 201–215; doi: 10.1130/B30559.1; 10 figures; 3 tables; Data Repository item 2013023.

decreases exponentially with depth through Earth's surface, such that at a depth of ~2 m in rock, little ^{10}Be is created through spallogenic reactions; muon-induced reactions continue to depths of tens of meters but at a much lower production rate. Thus, by sampling the uppermost portion of an outcrop and assuming steady and uniform erosion, the concentration of ^{10}Be reflects the time required for material to pass through the uppermost several meters of rock and regolith (Lal, 1991); this is the basis of erosion rate calculations.

During the past decade, hundreds of ^{10}Be measurements have been made on sediment samples collected from various streams and rivers near and within the central Appalachian Mountains, including drainage basins of different sizes in Shenandoah National Park (n = 37; Duxbury, 2009), the Susquehanna River Basin (n = 79; Reuter, 2005), and the Potomac River Basin (n = 62; Trodick, 2011). Paleo-erosion rates of contributing drainage basins to the New River in West Virginia were inferred from ^{10}Be and ^{26}Al concentrations in sediments deposited in caves (Granger et al., 1997). Basin-averaged erosion rates from these studies are low, with means averaging from 10 to 27 m m.y.$^{-1}$ for sampled drainages in our study area. Incision rates of the New River (Ward et al., 2005) and of the Potomac and Susquehanna River (Reusser et al., 2006) were inferred from measurements of ^{10}Be; such incision rates are reflective of only a single site, not erosion throughout each basin.

It is important to consider that basin-averaged erosion rates (Bierman and Steig, 1996; Brown et al., 1995; Granger et al., 1996) are not representative of the relatively small area occupied by ridgeline bedrock outcrops, nor are the processes by which rivers erode their basins the same as those by which outcrops lose mass. In fact, very few studies address the processes by which mass is lost from outcrops, though the effect of episodic removal of thick rock slabs from outcrops has been both modeled and measured (e.g., Bierman and Caffee, 2002; Lal, 1991; Small et al., 1997; Wakasa et al., 2006). In temperate climates, such as the central Appalachian Mountains, some bedrock erosion along ridgelines has been attributed not to contemporary processes but to periglacial activity during periods of colder climate, including enhanced freeze-thaw action and frost-heaving (Braun, 1989, 1993).

Prior to this study, 17 bedrock outcrop erosion rates had been published for the central Appalachian Mountains, including data from samples collected along ridges and summits in Shenandoah National Park (n = 5; Duxbury, 2009), the Susquehanna River Basin (n = 4; Reuter, 2005), and the Dolly Sods region of West Virginia (n = 8; Hancock and Kirwan, 2007). All three studies report low rates of outcrop erosion with means ranging from 4 to 7 m m.y.$^{-1}$.

This study presents 72 new ^{10}Be-based bedrock outcrop erosion rates from a variety of locations within the central Appalachian Mountains, specifically the Susquehanna River Basin (n = 26) and the Potomac River Basin (n = 46; Fig. 1); 62 of the 72 samples come from main ridgelines. The size of this new central Appalachian bedrock outcrop ^{10}Be erosion rate data set and the spatial distribution of these data allow us to test for relationships among erosion rates and climatic and topographic parameters. By measuring the rate of bedrock outcrop erosion, we can better assess the processes influencing modeled erosion rates (e.g., block removal and periglacial activity) and discuss the relationship between the ridgeline and basin-averaged erosion rates, which is prerequisite to understanding large-scale landscape change on millennial time scales.

Geographic and Geologic Setting

The central Appalachian Mountains are a dominant physiographic feature inland of eastern North America's Atlantic passive margin. This linear mountain chain extends 2500 km from the subpolar Canadian Maritime Provinces to humid, subtropical southern Georgia (Fig. 1, inset). The range is several hundred kilometers wide and generally steep, forested, and soil mantled, except along the highest ridgelines, where bedrock outcrops are common.

Five physiographic provinces are defined in and along the Appalachian Mountains (Fig. 1; Table 1). The undeformed sedimentary rock making up the Appalachian Plateau forms the western margin of the range. Further east, the highly deformed Valley and Ridge Province consists of a series of plunging anticlines and synclines of sedimentary rock. The Blue Ridge is a topographic feature held up in places by resistant units of quartz arenite and metamorphic quartzite extending from the Blue Ridge Escarpment in the south to just north of the Maryland-Pennsylvania border. The rolling Piedmont is underlain by high-grade metamorphic rocks. To the east, the low-lying Atlantic Coastal Plain exposes fluvial and shoreline sediments.

Rocks underlying the Appalachian Mountains have been deformed to varying degrees in numerous orogenic events. The most recent event, the Alleghenian orogeny, occurred throughout the Permian and was followed by Triassic rifting (Pazzaglia and Brandon, 1996; Poag and Sevon, 1989), which led to regional uplift (Pazzaglia and Gardner, 1994). Prior to rifting, Devonian sedimentary sequences were deposited in a foreland basin and now underlie the Valley and Ridge Province (Roden, 1991). In the Valley and Ridge Province, highly deformed, plunging anticlines and synclines trend parallel to the post-Alleghenian rift margin, exposing sandstones and arenites along the ridges and limestones and shales beneath the valleys. Post-Jurassic denudation rates throughout the region, as determined by long-term sediment budgeting as well as (U-Th)/He and fission-track thermochronologies, have fluctuated but on average remain low (~21 m m.y.$^{-1}$; Blackmer et al., 1994; Boettcher and Milliken, 1994; C.W. Naeser et al., 2001, 2005; N.D. Naeser et al., 2004; Pazzaglia and Brandon, 1996; Reed et al., 2005; Sevon, 1989; Spotila et al., 2004).

Over the Quaternary, continental ice sheets affected the northern Appalachian Mountains, advancing and retreating numerous times. At its farthest extent, ice covered the northern reaches of the Susquehanna River Basin (Fig. 1). Though the southern Appalachian Mountains were not directly affected by glaciation, the climate was cooler and drier during glaciations than it is today, and at least some of the ridgelines were affected by periglacial activity during cold phases (Braun, 1989).

METHODS

Field and Laboratory Methods

We located outcrops of quartz-rich lithologies based upon lithologic descriptions provided in bedrock geology maps downloaded from the U.S. Geological Survey (USGS) Geological Map Database (Fig. 1; Table 1; http://ngmdb.usgs.gov/) for Maryland, Pennsylvania, Virginia, and West Virginia. We cross-referenced names of sampling sites with gazetteers, topographic maps, and internet photos to assess the quality and accessibility of bedrock outcrops prior to field work.

Between two and four individual outcrop samples were collected from each of 26 sampling sites to test erosion rate variability at the outcrop scale; samples at each site were collected meters to tens of meters apart from one another (GSA Data Repository).[1] We collected samples that fall into two categories: main ridgeline outcrops (n = 62) and spur ridge outcrops (n = 10). Main ridgeline samples are those from outcrops along the highest local topographic feature. Spur ridge outcrops are those from a ridge angling down and away from the main ridgeline (Figs. 2A–2C).

[1]GSA Data Repository item 2013023, detailed description of field, laboratory, and accelerator mass spectrometry preparation and analysis methods, is available at http://www.geosociety.org/pubs/ft2013.htm or by request to editing@geosociety.org.

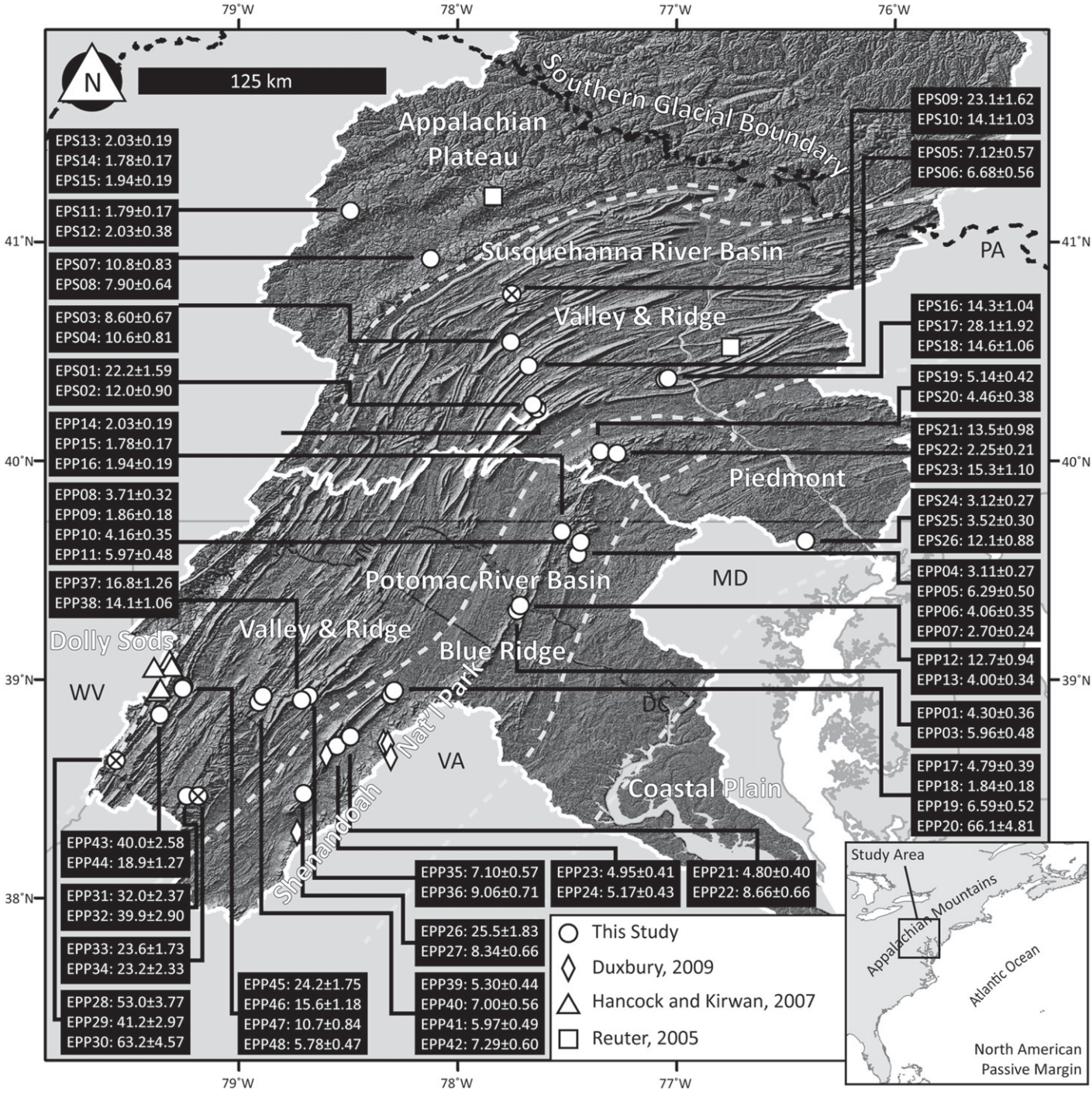

Figure 1. Bedrock outcrop sampling sites and ^{10}Be erosion rates (m m.y.$^{-1}$) in the Potomac (n = 46) and Susquehanna (n = 26) River Basins. White circles represent individual outcrop sites; white circles with an X indicate spur ridge samples that were excluded from all statistical analyses. All samples were collected south of the latest glacial limit. Samples come from four physiographic provinces: Blue Ridge (EPP01–EPP27 and EPS19–EPS23), Valley and Ridge (EPP28–EPP48, EPS01–EPS10, and EPS16–EPS18), the Appalachian Plateau (EPS11–EPS15), and the Piedmont (EPS24–EPS26). Specific coordinates for outcrop sites are listed in Table 1.

TABLE 1. SAMPLING SITES AND EROSION RATE DATA

Sample*	Sampling site†	Long. (°W)	Lat. (°N)	Elev. (masl)	Lithology	Thickness (cm)	Physiographic province#	LLNL Be ID§**	^{10}Be concentration (at g^{-1})††	Erosion rate (m m.y.$^{-1}$)§§	Average site erosion rate (m m.y.$^{-1}$)##	Deviation (m m.y.$^{-1}$)	RSD (%)***
Main ridgeline outcrops													
EPP01	Loudoun Heights, Harpers Ferry NHP, Virginia	77.736	39.310	349	Quartzite	3	BR	BE28738	762,174 ± 10,376	4.30 ± 0.36	5.13 ± 0.42	0.83	23
EPP02	″	77.737	39.310	350	Quartzite	2	BR	BE28739	581,777 ± 10,882	5.96 ± 0.48		0.83	
EPP04	White Rocks, Cunningham Falls SP, Maryland	77.453	39.569	415	Quartzite	5	BR	BE28740	1,239,538 ± 16,524	3.11 ± 0.27	4.04 ± 0.34	0.93	40
EPP05	″	77.454	39.568	433	Quartzite	5	BR	BE28741	678,285 ± 9175	6.29 ± 0.5		2.25	
EPP06	″	77.454	39.568	434	Quartzite	7	BR	BE28742	975,643 ± 14,832	4.06 ± 0.35		0.02	
EPP07	″	77.453	39.569	418	Quartzite	6	BR	BE28743	1,387,088 ± 19,597	2.70 ± 0.24		1.34	
EPP08	Chimney Rock, Catoctin Mountain Park, Maryland	77.432	39.629	407	Quartzite	2	BR	BE28744	1,023,955 ± 13,766	3.71 ± 0.32	2.79 ± 0.25	0.93	47
EPP09	″	77.433	39.629	419	Quartzite	2	BR	BE28745	1,807,331 ± 24,061	1.86 ± 0.18		0.93	
EPP10	Wolf Rocks, Catoctin Mountain Park, Maryland	77.438	39.633	419	Phyllite	5	BR	BE28746	949,718 ± 13,178	4.16 ± 0.35	5.07 ± 0.42	0.90	25
EPP11	″	77.438	39.632	394	Phyllite	3	BR	BE28747	687,367 ± 9572	5.97 ± 0.48		0.91	
EPP12	Maryland Heights, Harpers Ferry NHP, Maryland	77.716	39.341	438	Quartzite	3	BR	BE28749	362,136 ± 5128	12.65 ± 0.94	8.33 ± 0.64	4.33	73
EPP13	″	77.716	39.342	429	Quartzite	2	BR	BE28750	994,782 ± 13,387	4.00 ± 0.34		4.33	
EPP14	Raven Rock, South Mountain SP, Maryland	77.524	39.676	524	Quartzite	4	BR	BE28751	3,227,709 ± 36,079	1.00 ± 0.11	3.67 ± 0.31	2.67	98
EPP15	″	77.524	39.677	544	Quartzite	4	BR	BE28752	1,724,318 ± 19,298	2.25 ± 0.21		1.42	
EPP16	″	77.525	39.675	527	Quartz vein	4	BR	BE28753	596,762 ± 10,548	7.77 ± 0.62		4.10	
EPP17	Buzzards Rock, George Washington NF, Virginia	78.309	38.926	607	Arenite	6	BR	BE28754	719,083 ± 8341	4.79 ± 0.39	4.41 ± 0.36	0.38	54
EPP18	″	78.308	38.930	547	Arenite	3	BR	BE28755	1,890,539 ± 16,028	1.84 ± 0.18		2.57	
EPP19	″	78.303	38.940	396	Arenite	6	BR	BE28756	537,240 ± 6758	6.59 ± 0.52		2.18	
EPP21	Kennedy Peak, George Washington NF, Virginia	78.488	38.742	782	Arenite	2	BR	BE28758	843,731 ± 9030	4.80 ± 0.4	6.73 ± 0.53	1.93	41
EPP22	″	78.487	38.742	770	Arenite	3	BR	BE28760	499,925 ± 5413	8.66 ± 0.66		1.93	
EPP23	Duncan Knob, George Washington NF, Virginia	78.551	38.698	793	Arenite	7	BR	BE28761	922,879 ± 14,288	4.95 ± 0.41	5.06 ± 0.42	0.11	3
EPP24	″	78.551	38.698	788	Arenite	6	BR	BE28762	894,780 ± 15,205	5.17 ± 0.43		0.11	
EPP26	Cub Run, George Washington NF, Virginia	78.700	38.479	861	Sandstone	3	BR	BE28763	222,770 ± 3413	25.52 ± 1.83	16.93 ± 1.25	8.59	72
EPP27	″	78.700	38.480	851	Sandstone	5	BR	BE28764	636,487 ± 7881	8.34 ± 0.66		8.59	
EPP31	Reddish Knob, George Washington NF, Virginia/ West Virginia	79.240	38.470	1282	Sandstone	2	VR	BE28768	236,794 ± 4004	32.00 ± 2.37	35.97 ± 2.64	3.97	16
EPP32	″	79.240	38.470	1290	Sandstone	4	VR	BE28769	189,164 ± 2871	39.94 ± 2.9		3.97	
EPP35	Big Schloss Mtn., George Washington NF, Virginia/ West Virginia	78.682	38.926	881	Arenite	2	VR	BE28773	700,239 ± 9986	7.10 ± 0.57	8.08 ± 0.64	0.98	17
EPP36	″	78.680	38.925	864	Arenite	4	VR	BE28774	619,703 ± 8695	9.06 ± 0.71		0.98	
EPP37	Devil's Hole Mtn., George Washington NF, Virginia/ West Virginia	78.713	38.907	759	Sandstone	2	VR	BE28775	338,201 ± 5665	16.83 ± 1.26	15.45 ± 1.16	1.39	13
EPP38	″	78.713	38.907	776	Sandstone	4	VR	BE28776	393,756 ± 5593	14.06 ± 1.06		1.39	
EPP39	Crannys Crow, Lost River SP, West Virginia	78.906	38.901	876	Sandstone	3	VR	BE28777	965,199 ± 13,391	5.30 ± 0.44	6.15 ± 0.50	0.85	20
EPP40	″	78.905	38.902	875	Sandstone	5	VR	BE28778	743,899 ± 10,369	7.00 ± 0.56		0.85	
EPP41	Miller Rock, Lost River SP, West Virginia	78.894	38.916	951	Sandstone	8	VR	BE28779	888,805 ± 14,872	5.97 ± 0.49	6.63 ± 0.55	0.66	14
EPP42	″	78.894	38.915	949	Sandstone	2	VR	BE28780	776,198 ± 16,752	7.29 ± 0.6		0.66	
EPP43†††	Seneca Rocks, Monongahela NF, West Virginia	79.366	38.836	736	Sandstone	3	VR	BE28782	93,624 ± 1724	40.04 ± 2.58	29.49 ± 1.93	10.55	51
EPP44†††	″	79.366	38.836	730	Sandstone	4	VR	BE28783	183,484 ± 2755	18.94 ± 1.27		10.55	
EPP45	Chimney Rocks, Monongahela NF, West Virginia	79.255	38.973	952	Sandstone	3	VR	BE28784	253,346 ± 3185	24.16 ± 1.75	14.07 ± 1.06	10.09	56
EPP46	″	79.255	38.973	944	Sandstone	4	VR	BE28785	377,968 ± 6115	15.60 ± 1.18		1.53	
EPP47	″	79.259	38.964	927	Sandstone	1	VR	BE28786	509,193 ± 10,478	10.73 ± 0.84		3.34	

(*continued*)

TABLE 1. SAMPLING SITES AND EROSION RATE DATA (*continued*)

Sample*	Sampling site†	Long. (°W)	Lat. (°N)	Elev. (masl)	Lithology	Thickness (cm)	Physiographic province#	LLNL Be ID§**	^{10}Be concentration (at g^{-1})††	Erosion rate (m m.y.$^{-1}$)§§	Average site erosion rate (m m.y.$^{-1}$)##	Deviation (m m.y.$^{-1}$)	RSD (%)***
Main ridgeline outcrops (*continued*)													
EPP48	〃	79.259	38.963	920	Sandstone	1	VR	BE28787	887,092 ± 10,346	5.78 ± 0.47		8.29	
EPS03	Round Top Trail, Tuscarora SF, Pennsylvania	77.655	40.258	594	Sandstone	3	VR	BE28790	532,807 ± 7666	8.60 ± 0.67	9.59 ± 0.74	0.99	15
EPS04	〃	77.656	40.258	603	Sandstone	1	VR	BE28791	473,664 ± 6841	10.58 ± 0.81		0.99	
EPS05	Pine Ridge Trail, Tuscarora SF, Pennsylvania	77.678	40.436	509	Conglomerate	1	VR	BE28793	654,878 ± 9347	7.12 ± 0.57	6.90 ± 0.57	0.22	5
EPS06	〃	77.678	40.436	507	Conglomerate	1	VR	BE28794	692,283 ± 16,875	6.68 ± 0.56		0.22	
EPS07	Prayer Rock, Pennsylvania	77.757	40.544	583	Sandstone	3	VR	BE28795	427,397 ± 7287	10.83 ± 0.83	9.37 ± 0.74	1.47	22
EPS08	〃	77.758	40.543	585	Sandstone	2	VR	BE28796	570,167 ± 12,370	7.90 ± 0.64		1.47	
EPS11	Turtle Rocks, Moshannon SF, Pennsylvania	78.124	40.924	571	Sandstone	2	AP	BE28799	2,177,021 ± 23,048	1.79 ± 0.17	3.18 ± 0.28	1.39	62
EPS12	〃	78.124	40.924	571	Sandstone	4	AP	BE28800	981,990 ± 10,480	4.57 ± 0.38		1.39	
EPS13	Panther Rocks, Moshannon SF, Pennsylvania	78.491	41.142	681	Sandstone	2	AP	BE28801	2,111,813 ± 22,366	2.03 ± 0.19	1.92 ± 0.18	0.11	7
EPS14	〃	78.490	41.142	674	Sandstone	2	AP	BE28802	2,346,996 ± 32,353	1.78 ± 0.17		0.14	
EPS15	〃	78.490	41.143	672	Sandstone	1	AP	BE28804	2,207,321 ± 29,862	1.94 ± 0.19		0.02	
EPS16	Hawk Rock, Duncannon, Pennsylvania	77.055	40.370	367	Sandstone	2	VR	BE28805	284,989 ± 4041	14.32 ± 1.04	19.02 ± 1.34	4.70	41
EPS17	〃	77.045	40.374	346	Sandstone	7	VR	BE28806	148,005 ± 2195	28.13 ± 1.92		9.11	
EPS18	〃	77.041	40.376	323	Sandstone	3	VR	BE28807	277,083 ± 3952	14.62 ± 1.06		4.40	
EPS19	Michaux Oaks Rd., Michaux SF, Pennsylvania	77.348	40.043	488	Schist	2	BR	BE28808	807,132 ± 11,150	5.14 ± 0.42	4.80 ± 0.40	0.34	10
EPS20	〃	77.348	40.043	488	Schist	4	BR	BE28809	899,523 ± 13,270	4.46 ± 0.38		0.34	
EPS21	Pole Steeple, Michaux SF, Pennsylvania	77.267	40.032	403	Quartzite	4	BR	BE28810	296,452 ± 4139	13.52 ± 0.98	10.35 ± 0.76	3.17	68
EPS22	〃	77.267	40.033	406	Quartzite	5	BR	BE28811	1,362,536 ± 16,589	2.25 ± 0.21		8.10	
EPS23	〃	77.267	40.033	407	Quartzite	5	BR	BE28812	264,200 ± 3703	15.27 ± 1.1		4.92	
EPS24	Rock Ridge, Rocks SP, Maryland	76.413	39.635	160	Schist	4	P	BE28813	950,218 ± 10,464	3.12 ± 0.27	6.24 ± 0.48	3.12	81
EPS25	〃	76.413	39.636	157	Schist	2	P	BE28815	871,716 ± 9605	3.52 ± 0.3		2.72	
EPS26	〃	76.413	39.635	162	Quartz vein	5	P	BE28816	297,170 ± 4141	12.09 ± 0.88		5.85	
Spur ridge outcrops													
EPP20	Buzzards Rock, George Washington NF, Virginia	78.299	38.945	333	Sandstone	2	BR	BE28757	66,938 ± 2369	66.10 ± 4.81			
EPP28	Sawmill Run Rd., Monongahela NF, West Virginia	79.561	38.629	836	Sandstone	2	VR	BE28765	129,322 ± 2254	53.03 ± 3.77			
EPP29	〃	79.561	38.628	851	Sandstone	2	VR	BE28766	164,689 ± 3031	41.18 ± 2.97			
EPP30	〃	79.560	38.629	867	Sandstone	2	VR	BE28767	109,250 ± 2533	63.21 ± 4.57			
EPP33	Hone Quarry Ridge, George Washington NF, Virginia	79.191	38.466	836	Sandstone	2	VR	BE28771	263,844 ± 4292	23.58 ± 1.73			
EPP34	〃	79.185	38.464	809	Sandstone	3	VR	BE28772	195,350 ± 3454	32.24 ± 2.33			
EPS01	Rim Trail, Tuscarora SF, Pennsylvania	77.642	40.235	574	Sandstone	6	VR	BE28788	230,861 ± 3456	22.19 ± 1.59			
EPS02	〃	77.641	40.235	578	Sandstone	4	VR	BE28789	410,871 ± 5972	11.99 ± 0.9			
EPS09	Spring Creek, Rothrock SF, Pennsylvania	77.755	40.763	416	Sandstone	7	VR	BE28797	199,788 ± 2910	23.10 ± 1.62			
EPS10	〃	77.755	40.763	419	Sandstone	2	VR	BE28798	323,549 ± 4464	14.09 ± 1.03			

*Samples named EPPxx, where "xx" is the sample number from the Potomac River Basin. Samples labeled EPSxx come from the Susquehanna River Basin.

†NHP—National Historical Park; SP—State Park; NF—National Forest; SF—State Forest.

§Elevation data were taken from the National Elevation Dataset (ned.usgs.gov). Resolution of 1/3 arcsecond (10 m).

#Physiographic region as specified by the U.S. Geological Survey (http://tapestry.usgs.gov/physiogr/physio.html): AP—Appalachian Plateau; VR—Valley and Ridge; BR—Blue Ridge; P—Piedmont.

**Identification reference number for each sample within the sample database at the Center for Mass Spectrometry at Lawrence Livermore National Laboratory, Livermore, California. Samples were analyzed in April 2010.

††Normalized using the ICN standard solution, 07KNSTD3110 with a reported ratio of 2.85 ×10^{-12} (Nishiizumi et al., 2007). Reported errors are 1σ accelerator mass spectrometry (AMS) measurement uncertainties. Blank corrections average 4% of measured Be ratios.

§§Erosion rates estimated using the CRONUS online cosmogenic calculator (Balco et al., 2008). Calculator version 2.1 was used and incorporates equation constants version 2.2.1 and accounts for muogenic production of ^{10}Be with the muon script version 1.1. An assumed rock density of 2.7 g cm^{-3} is used in our calculations.

##Values are for each sampling site.

***Relative standard deviation.

†††EPP43 and EPP44 were collected from a site with horizon blocking of incoming cosmic rays. Erosion rates in the table are calculated using a shielding-corrected production rate (Dunne et al., 1999).

We sampled from two physiographic provinces in the Potomac River Basin and from four in the Susquehanna River Basin. Our samples come from the Appalachian Plateau (n = 5), the Valley and Ridge (n = 34), the Blue Ridge (n = 30), and the Piedmont (n = 3). The three Piedmont samples and five Appalachian Plateau samples are all within the Susquehanna River Basin, as no suitable bedrock outcrops were accessible in the Potomac River Basin during our field season.

Samples were returned to the University of Vermont, where they were processed to obtain purified quartz following the methods of Kohl and Nishiizumi (1992). The quartz from each sample and a known amount of ^{9}Be carrier solution were digested in concentrated HF, and Be was subsequently separated from Fe, Al, Ti, and B. Specific quartz-preparation methods can be found at the University of Vermont Cosmogenic Nuclide Laboratory Web site (http://www.uvm.edu/cosmolab/?Page = methods.html).

The ^{10}Be/^{9}Be ratios were measured by accelerator mass spectrometry (AMS) at Lawrence Livermore National Laboratory in April 2010. All samples were normalized to standard 07KNSTD3110, with a reported ^{10}Be/^{9}Be ratio of 2.85×10^{-12} (Nishiizumi et al., 2007). The ^{10}Be concentrations were derived from these ^{10}Be/^{9}Be ratios and used to calculate erosion rates using the CRONUS online cosmogenic erosion rate calculator (version 2.2; Balco et al., 2008). We used production rates corrected for latitude and elevation based on the scaling schemes of Lal (1991) and Stone (2000). Results are normalized to a high-latitude and sea-level ^{10}Be production rate of 4.96 ± 0.43 atoms g^{-1} yr^{-1} (Balco et al., 2008). Errors reported in our analyses are 1σ AMS measurement errors and are propagated through the CRONUS calculations.

Parametric Statistics

Parametric statistical analyses assume a normal distribution of data. To test for normality, we ran a Shapiro-Wilkes W analysis, which tests the null hypothesis that erosion rates fit a normal distribution. The initial test on our data failed ($p < 0.01$; Fig. 3), and therefore we log-transformed (base 10) the erosion rates. The distribution of log-transformed erosion rates passed the Shapiro-Wilkes W analysis ($p = 0.71$, Fig. 3, inset). All nonspatial statistical analyses were performed using the log-transformed erosion rate data.

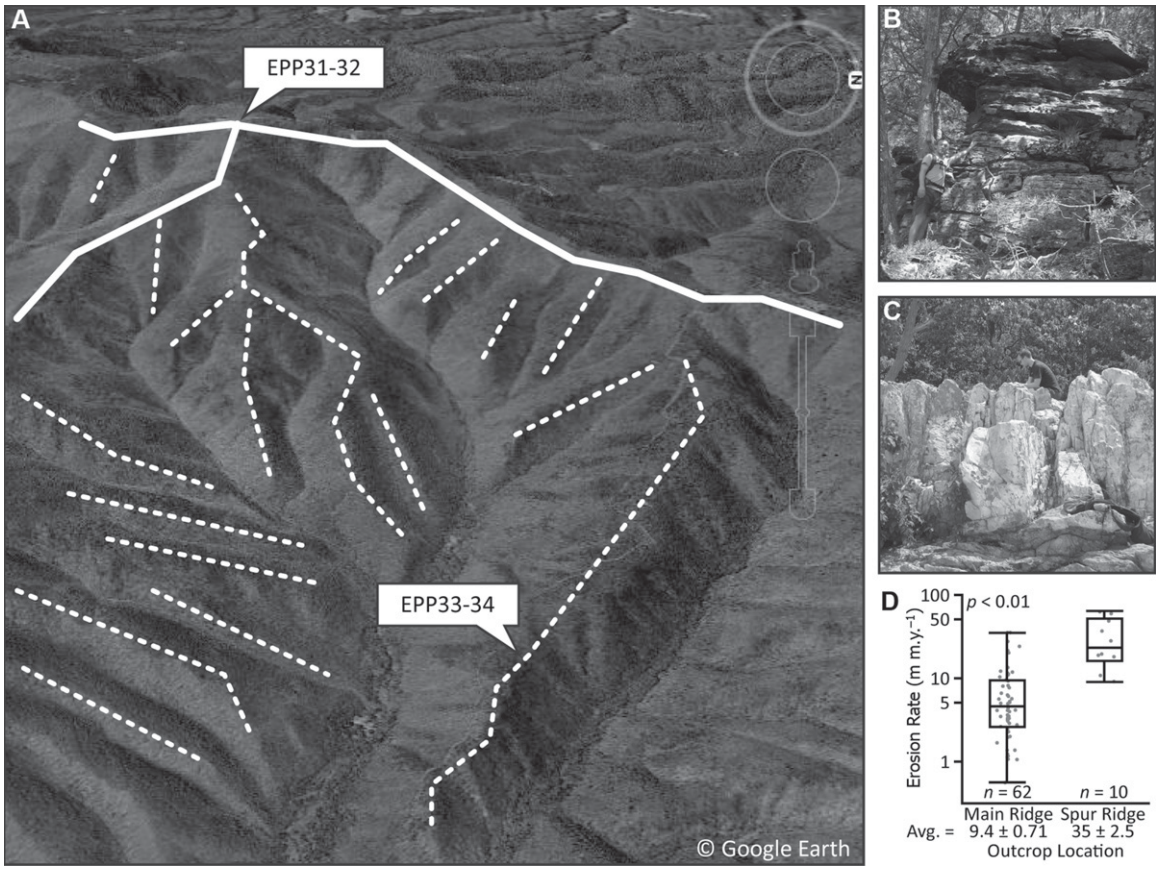

Figure 2. (A) Aerial photograph from Google Earth depicting our classification of main ridgelines (solid lines) and spur ridges (dashed lines). The words "© Google Earth" are 1 km. (B) Photograph of a spur ridge outcrop (EPP34), a sandstone outcrop on Hone Quarry Ridge in George Washington National Forest, Virginia. (C) Photograph of a ridgeline outcrop (EPS22), a quartzite outcrop at Pole Steeple in Michaux State Forest, Pennsylvania. (D) Box and whisker plots depicting the data used in a Student's *t*-test comparison of the means of main ridgeline outcrop erosion rates to the mean of spur ridge erosion rates, which are significantly different ($p < 0.01$). The ends of the whiskers denote the range of erosion rates in each category, while the top, middle, and bottom of each box mark the 75th, 50th, and 25th percentiles, respectively. Gray dots represent individual erosion rate samples.

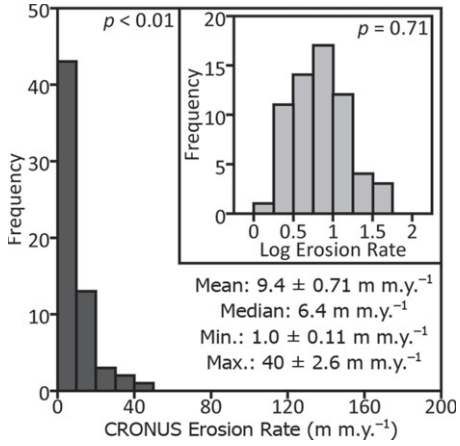

Figure 3. Frequency distribution of measured outcrop erosion rates from main ridgelines (*n* = 62) calculated using the CRONUS online calculator (Balco et al., 2008). *P*-values using a Shapiro-Wilkes W test for normality for each distribution are provided. After log-transformation, erosion rates form a normal distribution (inset).

We analyzed bivariate relationships among sample erosion rates and physical and environmental parameters (Table 1; Table A1 [see footnote 1]) such as latitude (°N), elevation (m above sea level [asl]), relief (m in a 50 m radius of the outcrop), and mean annual precipitation (MAP, mm yr^{-1}; Hijmans et al., 2005) and temperature (MAT, °C; Hijmans et al., 2005). We performed a multivariate standard least-squares regression; however, we recognize that our chosen environmental parameters are, in some cases, correlated with one another and thus performed a principal component analysis (PCA) to ensure that a line of best fit through our erosion rates was regressed through independent variables.

We used three statistical tests to compare the means of subgroups of data categories: analysis of variance (ANOVA), Tukey-Kramer honestly significant difference (HSD), and Students *t*-test. ANOVAs were used to determine the similarity of mean values between multiple groups. Tukey-Kramer HSD tests compared every possible pairing of groups from the ANOVA to determine which groups were statistically similar or dissimilar from one another. We performed these two methods for each set of categorical data (e.g., lithology) to determine whether the mean erosion rates of subgroups within each category (e.g., quartzite, sandstone, schist, etc.) were statistically similar. Just as we used an ANOVA to determine if the means of more than two groups of data were similar or dissimilar, we used a Student's *t*-test to determine if means of two groups of data were similar or not (e.g., erosion rates from outcrops in the Potomac River Basin vs. those in the Susquehanna River Basin).

Spatial Statistics

We use several statistics to understand how erosion rates are spatially related. At the individual outcrop scale, we calculated the deviation of each sample to determine the spread of erosion rates at each sampling site. We then generalized the deviation at each site using the relative standard deviation (RSD) of erosion rates.

Different methods were needed to ascertain spatial patterns in our data across the entire field area. We tested the spatial autocorrelation of erosion rates using a semivariogram analysis developed and coded in Matlab (version 7.10.0, release 2010a). In the geostatistical literature, semivariance, $\gamma(h)$, is used to describe spatial patterns between measured observations as a function of the separation distance. These patterns are usually described in terms of dissimilarity rather than similarity (or correlation). The spatial dissimilarity between observations separated by a distance h may be defined as:

$$\gamma(h) = \frac{1}{2N(h)} \sum_{i=1}^{N(h)} \left[u(a)_i - u(a+h)_i\right]^2, \quad (1)$$

where $N(h)$ is the number of data pairs separated by the distance h, and $u(a)$ and $u(a + h)$ are the parameter values at locations (a) and some distance ($a + h$) away (Issaks and Srivastava, 1989; Journel and Huijbregts, 1978).

The semivariogram plots the calculated variance between erosion rates from any two outcrops against the distance between those outcrops (Fig. 4A). Paired data are then separated into bins (Fig. 4B); the average variance for all paired data points in each bin is plotted as a single point along the *y*-axis. The resulting plot is known as the experimental semivariogram (Fig. 4B). This experimental semivariogram is best fit by a model semivariogram that describes the spatial structure (range of spatial autocorrelation) of the data defined by three model parameters—the nugget, sill, and range (Fig. 4C). The *nugget* is the projected discontinuity shown at the origin of the plot; it represents both the measured parameter error (in our case, error associated with collecting samples, measuring ^{10}Be concentrations, and inferring erosion rates) as well as the spatial sources of variation at distances smaller than the shortest distance between samples (Journel and Huijbregts, 1978). For example, given no sampling or laboratory error, two erosion rate measurements taken from a fixed location at the top of the same outcrop should erode similarly, and the nugget would be 0. The *range* (referred to as the decorrelation distance) defines the distance at which the variable is no longer spatially autocorrelated. The semivariance associated with the model plateau is defined as the *sill*. It is possible for the variable in question to become spatially autocorrelated again at larger distances (i.e., where average bin values begin to increase consistently above the sill), resulting in a model semivariogram with multiple decorrelation distances.

Horizon Shielding Corrections

Samples from the top of an outcrop receive full cosmic-ray bombardment from the open sky, whereas those from sites that are shadowed or obstructed by other objects receive only a fraction of the total potential-cosmic ray bombardment. A shielding factor must be applied to samples collected from such sites before an erosion rate can be appropriately inferred (Dunne et al., 1999; Lal, 1991). Samples EPP43 and EPP44 were collected from a horizontal surface ~1 m away from an ~3-m-high vertical slab of rock at Seneca Rocks, in West Virginia. We used the methods of Dunne et al. (1999) to obtain an estimated shielding factor of ~0.575 for these two samples, which we applied before using CRONUS to determine an erosion rate for each sample.

RESULTS

All 72 samples contained large amounts of ^{10}Be, ranging from 6.69×10^4 to 3.23×10^6 atoms g^{-1}. Such ^{10}Be concentrations indicate that sampled outcrops integrate cosmic-ray dosing over more than 10^4 to nearly 10^6 yr. Concentrations of ^{10}Be can be interpreted as outcrop exposure ages, assuming the outcrop erosion rate is negligible, or as outcrop erosion rates, assuming mass loss is constant and steady (Lal, 1991). Because field observations show signs of active mass loss from the sampled outcrops (e.g., granular disintegration, spalling of thin sheets of rock, loosening of rock slabs), we interpret the ^{10}Be concentration data as rates of erosion. In reality, the episodic loss of slabs of rock from at least some outcrops means that measured ^{10}Be concentrations reflect both the rate of erosion and the time since the last slab of rock peeled off the outcrop.

Bedrock outcrop erosion rates modeled from our measured ^{10}Be concentrations range from 1.0 to 66 m m.y.$^{-1}$ for samples from both main ridgelines and spur ridges. The average erosion rate for outcrops on main ridgelines from the entire field area is 9 ± 1 m m.y.$^{-1}$ (n = 62; 1σ standard deviation; Table 1). The distribution of main ridgeline erosion rates is skewed to the left; the median rate of outcrop erosion is 6.4 m m.y.$^{-1}$ (Fig. 3). Spur ridge outcrops erode at an average

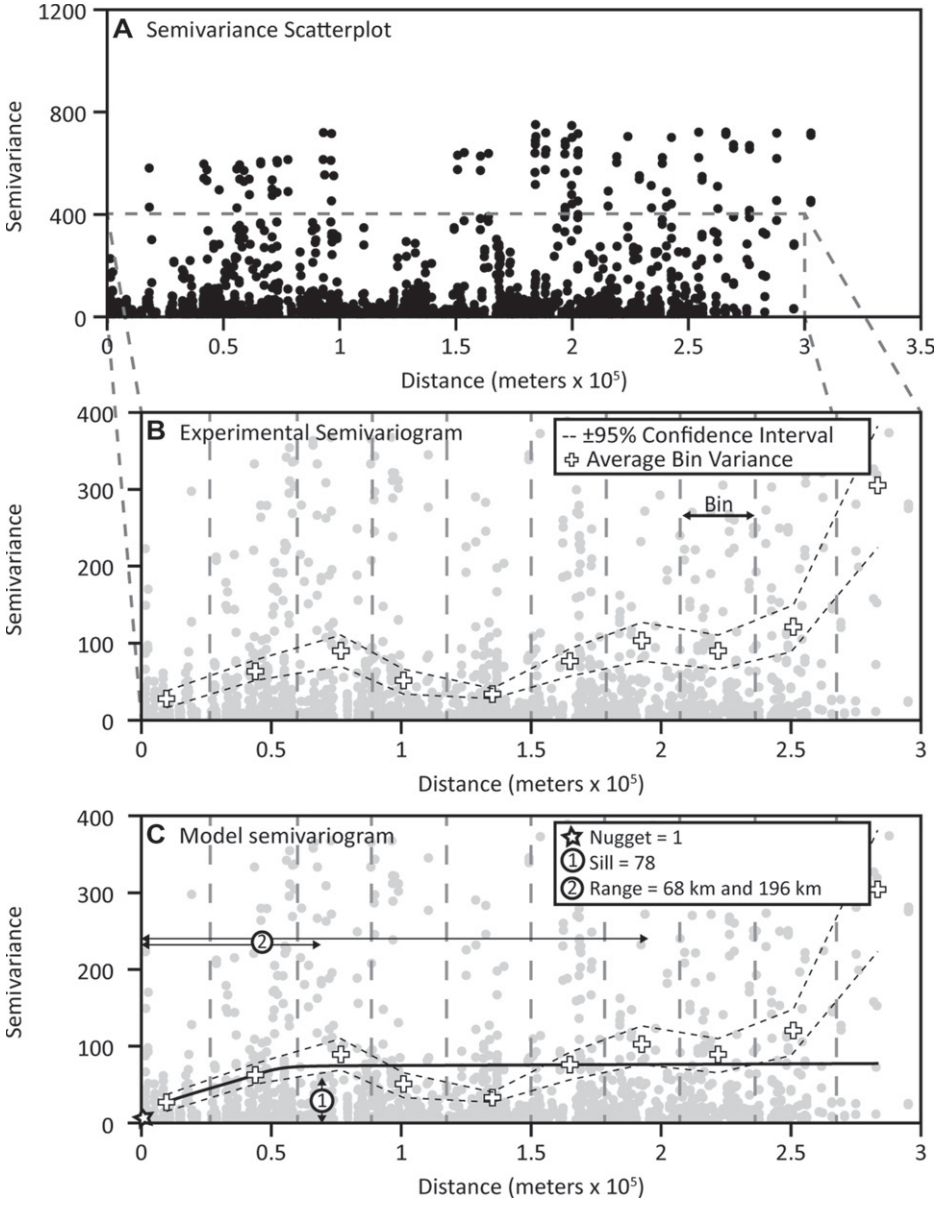

Figure 4. Results from a semivariogram analysis of spatial autocorrelation within the outcrop erosion rate data. (A) The variance between erosion rates from any given outcrop sample and all other outcrop samples plotted against the separation distance between any two samples. (B) Variance values associated with paired data are grouped into ten bins of equal population and an experimental semivariogram is produced by plotting the average variance for each bin, represented by the white plus signs; the dotted lines represent the 95% confidence interval of the average semivariance values. (C) An exponential model semivariogram best fits the experimental semivariogram, illustrating the spatial structure of the data using the nugget, sill, and range. This approach often yields one decorrelation distance; however, in our case, erosion rates are spatially autocorrelated at two distances.

rate of 35 ± 2.5 m m.y.$^{-1}$ (n = 10; Table 1) and have a median erosion rate of 27 m m.y.$^{-1}$.

A Student's t-test shows that outcrop erosion rates on spur ridges are significantly higher than those on main ridgelines ($p < 0.01$; Fig. 2D), implying the processes or the rates of processes controlling ^{10}Be concentration differ between ridgelines and spur ridges. Because our interest is comparing the rate of ridgeline lowering to that of drainage basins as a whole, the following results and statistics are based solely on erosion rates from main ridgeline outcrops.

Controls on Erosion Rates

Regression analyses of environmental and physical parameters show that no variables are strongly correlated with bedrock outcrop erosion rates, though weak correlations are observed between erosion rates and elevation, relief, and latitude (Table 2; Fig. A1 [see footnote 1]). An ANOVA shows that erosion rates do not significantly vary among climate zones ($p = 0.93$; Fig. 5A; Table 3), as defined by different temperature and precipitation combinations (Peel et al., 2007); neither temperature nor precipitation is significantly correlated to outcrop erosion rate alone (Table 2). An ANOVA comparing the means of quartzite (n = 15), sandstone (n = 28), arenite (n = 9), and schist (n = 4) outcrops indicates dissimilarity ($p = 0.01$; Fig. 5B; Table 3) and Tukey-Kramer HSD results show that sandstone outcrops erode faster than quartzite outcrops (Fig. 5D), but all other paired lithologies erode at statistically similar rates. We did not include samples from conglomerate, phyllite, or quartz vein outcrops because their sample populations were too small for a robust comparison (n = 2 for each).

PCA created new variables (i.e., principal components), each explaining a different amount of the erosion rate variance (Tables A2 and A3 [see footnote 1]). When used in a multivariate standard least-squares analysis, these new independent variables describe less than 25% of erosion rate variability throughout our field site ($R^2 = 0.22$, $p = 0.01$; Table 2).

Spatial Variance of Erosion Rates

Erosion rates of ridgeline outcrops are similar between the two basins (p = 0.53; Table 3; Fig. 5E). The range of bedrock outcrop erosion rates in the Potomac River Basin (1.0–40 m m.y.$^{-1}$; n = 40) is broader than that of bedrock outcrops in the Susquehanna River Basin (1.8–28 m m.y.$^{-1}$; n = 22), likely due to a larger sample population in the Potomac data set; the median outcrop erosion rates are also similar (6.1 and 6.9 m m.y.$^{-1}$, respectively) between the river basins (Fig. 5E; Table 3).

Outcrop erosion rates from the same physiographic provinces (i.e., Blue Ridge, Valley and Ridge) are also similar, even when spread across two separate drainage basins (Figs. 5C and 5F; Table 3). No comparison can be made for bedrock outcrops situated in the Appalachian Plateau or Piedmont Provinces because all samples for these provinces were collected within the Susquehanna River Basin. An ANOVA indicates statistically significant differences in the mean erosion rates from each province ($p < 0.01$; Fig. 5C), and the results from a Tukey-Kramer HSD

TABLE 2. REGRESSION RESULTS

Erosion rate versus ...		R^{2*}	*p* value
Elevation (masl)†	+	0.0684	0.04
Relief (m)†	+	0.0982	0.01
Mean annual precipitation (mm yr^{-1})§	+	0.0054	0.57
Mean annual temperature (°C)§	+	0.0003	0.89
Latitude (°N)	–	0.1327	0.00
Multivariate principal component analysis (PCA)		0.2233	0.01

*R^2 symbols tell whether the correlation is positive (+) or negative (–). Bivariate plots can be found in the GSA Data Repository (see text footnote 1).

†Relief is considered to be the change in elevation within a 50 m radius around each sampled outcrop. Elevation data were taken from the National Elevation Data Set (ned.usgs.gov). Resolution of 1/3 arcsecond (10 m).

§Mean annual precipitation and temperature data are from Hijmans et al. (2005).

analysis show that erosion rates from the Valley and Ridge are significantly higher than those from the Appalachian Plateau and those from the Blue Ridge ($p < 0.01$; Fig. 5D); otherwise, erosion rates from all other pairs of provinces are indistinguishable (Table 3).

RSDs from each sampling site cover a wide range (3%–98%; Table 1), with an average of 37% for 26 sampling sites. Erosion rates are more variable throughout our entire field area (108,000 km^2) than at individual sampling sites, as indicated by a large relative standard deviation based on all sampled outcrops (RSD = 93%). While the range of outcrop erosion rates through the field area is large (1.0–66 m m.y.$^{-1}$), the average deviation of any erosion rate from the mean of its sampling site is low (2.6 m m.y.$^{-1}$; Table 1).

Ridgeline samples (n = 62) yielded a total of 1892 unique distances between any two sampling sites throughout the entire field area. These pairs of data were grouped into ten bins of equal population size, and the average semivariance for each bin was calculated (Fig. 4B). The experimental semivariogram is best fit by an exponential model with two spatial ranges: one at 68 km and the other at 196 km (Fig. 4C). The nugget suggests that samples separated by a distance smaller than the closest two outcrops we sampled (~1 m) are more likely to produce erosion rates that vary up to 1 m m.y.$^{-1}$ from the average, a projected value not dissimilar to the observed average deviation of 2.6 m m.y.$^{-1}$.

DISCUSSION

The ^{10}Be concentrations measured in samples from ridgeline outcrops in the central Appalachian Mountains indicate low erosion rates

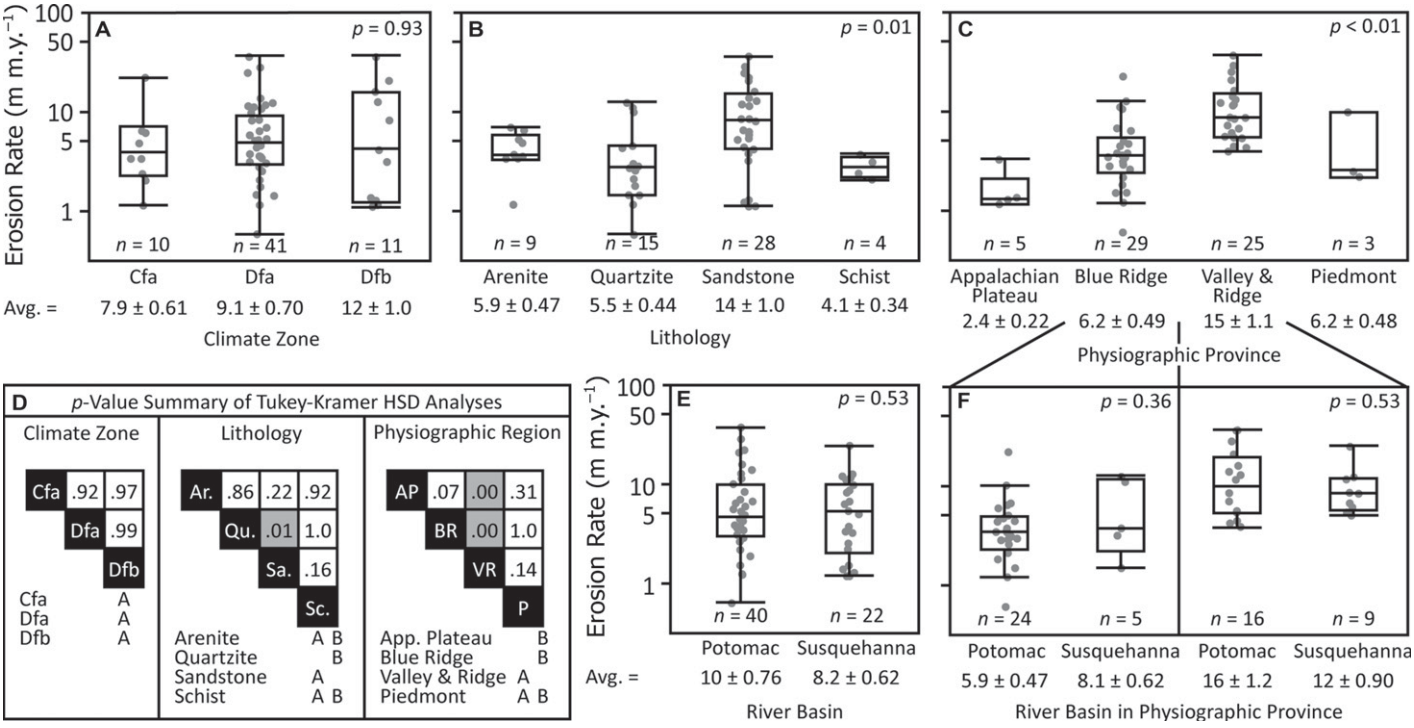

Figure 5. Box and whisker plots of outcrop erosion rates used in analysis of variance (ANOVA). The ends of the whiskers denote the range of erosion rates in each category, while the top, middle, and bottom of each box mark the 75th, 50th, and 25th percentiles, respectively. Gray dots represent individual erosion rate samples. (A) Climate zone, as classified by the Köppen-Geiger Classification system (Peel et al., 2007): Temperate climates have an annual high temperature >10 °C and an annual low temperature >0 °C but <10 °C; cold climates have an annual high temperature >10 °C and an annual low temperature of ≤0 °C; Cfa—Temperate: hot summer without dry season; Dfa—Cold: hot summer without dry season; Dfb—Cold: warm summer without dry season. (B) Outcrop lithology. Samples from quartz vein, phyllite, and conglomerate outcrops are not included because their sample populations are too small (n = 2). (C) Physiographic provinces of the central Appalachian Mountains from which samples were collected. (D) Results of paired analyses of Tukey-Kramer honestly significant difference (HSD) analyses of climate zones, lithologies, and physiographic provinces. (E) Outcrop erosion rates for the Susquehanna and Potomac River Basins. A Student's t-test indicates similarity between the two sample populations (p = 0.53). (F) Outcrop erosion rates from the Blue Ridge and Valley and Ridge Provinces of both the Potomac and Susquehanna River Basins. Erosion rates are not statistically different in either physiographic province.

TABLE 3. CATEGORIZED EROSION RATE STATISTICS

Outcrop erosion rate group	Sample population (*n*)	Mean erosion rate (m m.y.$^{-1}$)	Median erosion rate (m m.y.$^{-1}$)
All collected samples	72	12.93 ± 0.96	7.21
Spur ridge	10	35.07 ± 2.53	27.91
Main ridgeline	62	9.36 ± 0.71	6.44
Potomac River Basin	40	10.01 ± 0.76	6.13
Susquehanna River Basin	22	8.19 ± 0.62	6.90
Appalachian Plateau	5	2.42 ± 0.22	1.94
Blue Ridge	29	6.24 ± 0.49	4.80
Potomac Blue Ridge	24	5.85 ± 0.47	4.80
Susquehanna Blue Ridge	5	8.13 0.62	5.14
Piedmont	3	6.24 ± 0.48	3.52
Valley and Ridge	25	14.74 ± 1.09	10.73
Potomac Valley and Ridge	16	16.24 ± 1.19	12.40
Susquehanna Valley and Ridge	9	12.09 ± 0.90	10.58
Arenite	9	5.88 ± 0.47	5.17
Conglomerate	2	6.90 ± 0.57	6.90
Phyllite	2	5.07 ± 0.42	5.07
Quartzite	15	5.53 ± 0.44	4.00
Quartz vein	2	9.93 ± 0.75	9.93
Sandstone	28	13.74 ± 1.01	10.66
Schist	4	4.06 ± 0.34	3.99
Temperate: hot summer without dry season (Cfa)	10	7.93 ± 0.61	5.70
Cold: hot summer without dry season (Dfa)	41	9.12 ± 0.70	6.68
Cold: warm summer without dry season (Dfb)	11	11.58 ± 0.84	5.78
Global data set*	299	12.60 ± 1.37	5.47

*Bedrock outcrops in tectonically quiescent environments (from Portenga and Bierman, 2011).

(Fig. 3), best represented by the median erosion rate of 6 m m.y.$^{-1}$. Assuming steady erosion, these rates suggest that ^{10}Be measurements integrate over 10^4–10^6 yr of erosional history, which is the time it would take to remove several meters of rock from the sampled outcrops. Although erosion rates as high as a few tens of meters per million years exist within our data set, the majority of outcrops suggest that ridgelines within our study area are eroding slowly, and the time-averaged erosion rate determined by our 62 main ridgeline samples thus sets the pace for ridgeline lowering.

Influence of Outcrop Exposure History on Erosion Rates

We infer outcrop erosion rates from a measured quantity of ^{10}Be; however, we cannot accurately describe an outcrop's exact exposure history or quantify stochastic erosion processes that affect the interpretation of nuclide concentrations. A key assumption in the cosmogenic erosion rate methodology is that a sampled bedrock outcrop surface, once exposed to cosmic rays, continues to be bombarded at a constant rate while material is gradually removed from the outcrop. Sometimes, however, mass is often removed from an outcrop by the loss of large blocks or slabs (e.g., Bierman and Caffee, 2002; Small et al., 1997) or by landsliding (e.g., Niemi et al., 2005). When block-removal occurs and a sample is collected from a newly exposed rock surface, the inferred erosion rate will overestimate the time-averaged erosion rate; conversely, when a sample is collected from an outcrop that fails soon after the sample was removed, the inferred erosion rate may be underestimated (Lal, 1991; Small et al., 1997).

Small amounts of soil cover or colluvium can increase the rate at which bedrock erodes and reduce the production rate of ^{10}Be by absorbing some cosmic rays (Braun, 1989; Heimsath et al., 1997, 1999). Such cover creates conditions favorable for accelerated water-rock interactions, speeding the rate of erosion by processes including chemical weathering, freeze-thaw, frost-heave, and in periglacial environments, solifluction (Braun, 1989, 1993; Eaton et al., 2003; Heimsath et al., 1999). Some of these erosion processes are particularly active on periglacial hillslopes, where near-surface temperatures fluctuate around the freezing point (Delunel et al., 2010; Hales and Roering, 2007), a common occurrence in parts of the Potomac and Susquehanna River Basins during glacial periods (Peel et al., 2007).

Compared to main ridgeline outcrops, spur ridge outcrops (at lower elevations on hillslopes) are more susceptible to being covered by soil, sediment, and colluvium transported downslope from above. Intermittent burial of spur-ridge outcrops leads to conditions that both hasten rock erosion and also attenuate the cosmic-ray flux, reducing the ^{10}Be production rate, and thus the nuclide concentration in spur ridge samples.

Physical and Spatial Variables Influencing Outcrop Erosion Rates

Bivariate correlations between erosion rates and various parameters may be indicative of processes affecting the rate at which rock erodes and are useful when interpreting observations on a small spatial scale (Portenga and Bierman, 2011); however, bivariate correlations can be strongly affected by autocorrelation of variables, making causal attribution uncertain. Because such bivariate relationships are not independent of one another, interactions between variables are likely combined to affect erosion rates in ways we do not yet understand.

The bivariate correlation between erosion rate and relief is the strongest in our data set (Table 2) and has been observed in landscapes around the world (Montgomery and Brandon, 2002; Portenga and Bierman, 2011). We observe a weak bivariate correlation between erosion rate and elevation (Table 2). A similar relationship has been observed in regions with annual temperatures that fluctuate around the freezing point, such as the Appalachian Mountains, and this has been attributed to a higher likelihood of water-fed frost cracking (Hales and Roering, 2007; Portenga and Bierman, 2011).

Multivariate least-squares regression analyses of environmental variables only account for 22% of erosion rate variability (Table 2); therefore, unquantified rock properties (e.g., cementation, porosity, fracture density) and temporal factors such as response to base-level change, drainage migration, and local uplift may play significant roles in controlling bedrock outcrop erosion rates. For example, structural deformation of rock, and the resulting foliation and jointing, likely affects overall rock strength, consistent with our observation that outcrop erosion rates in the highly deformed Valley and Ridge Province are significantly higher than those in the undeformed Appalachian Plateau Province (Figs. 1 and 5C). Other rock properties such as cementation and rock strength may explain why we observe lower erosion rates in weathering-resistant quartzite outcrops of the Blue Ridge Province compared to the sandstone outcrops of the Valley and Ridge Province (Figs. 1 and 5C). Furthermore, stream capture separates sandstone-capped ridges, relicts of the retreating passive-margin escarpment, from the continental divide as it migrates landward through the Valley and Ridge, effectively lowering the base level of streams on all sides of these ridges (Gunnell and Harbor, 2010), possibly contributing to their higher rates of erosion.

We observe a decrease in erosion rates with an increase in latitude (Table 2), though it is not clear why. Some studies suggest that ero-

sion rates increase in regions closer to previous periglacial activity (Braun, 1989; Hales and Roering, 2007); however, on a global scale, outcrops in polar climates erode more slowly than those in temperate climates (Portenga and Bierman, 2011), leading one to expect lower outcrop erosion rates with increasing latitude. We investigated whether slower-eroding lithologies (i.e., schist, arenite, quartzite) were grouped at higher latitudes in our field area, but they are not; rather, sandstone outcrops have the largest latitudinal range of any lithology we sampled (~38°N–41°N). Among sandstone outcrops, there is a significant negative correlation between erosion rates and increasing latitude (n = 28; R^2 = 0.39; p < 0.01). No other lithology has as large a latitudinal spread, and none indicates any relationship between erosion rates and latitude.

During the Pleistocene, streams flowing toward the Atlantic Ocean broke through the Blue Ridge in Virginia, initiating a southwestern migration of the continental divide through the Valley and Ridge as the Susquehanna, Potomac, and James Rivers pirated stream catchments that had previously drained south to the Gulf of Mexico (e.g., Erickson and Harbor, 1998; Harbor et al., 2005; Naeser et al., 2001; Prince et al., 2010). Contemporaneously, the source of sediment in Mid-Atlantic offshore basins shifted to the south (e.g., Gunnell and Harbor, 2010; Poag and Sevon, 1989). While it is possible that our observed southerly increase in outcrop erosion rates reflects the southerly shift in sediment deposition, it is not likely, as basin-averaged erosion rates estimated with ^{10}Be from the Susquehanna and Potomac River Basins do not follow this trend but rather increase at higher latitudes (Reuter, 2005; Trodick, 2011).

The variability in erosion rates increases with distance between outcrop samples. For example, although the RSD calculated from all 62 main ridgeline outcrops is high (93%), the average RSD at our 26 individual sampling sites is much lower (37%), indicating that the erosion rate variability decreases when samples are separated by distances of only tens of meters, a finding consistent with the semivariogram analysis (Fig. 6). The range of sampling site RSDs is wide (3%–98%; Table 1), but because most erosion rates are low (median = 6 m m.y.$^{-1}$), the higher RSD values of some sampling sites (e.g., Chimney Rock in Catoctin Mountain Park, Buzzards Rock, Turtle Rocks) reflect erosion rate differences of only ~2–4 m m.y.$^{-1}$. Furthermore, the average deviation from the average erosion rate at any sampling site is only 2.6 m m.y.$^{-1}$; outcrops in the immediate vicinity of one another usually do not have very different erosion rates when considered in the absolute sense. The implications of this finding are significant in that a single outcrop sample represents reasonably well the erosion rate of an entire sampling site, though the overall erosion rate of a large region is best represented by a large sample population.

We infer—based on both isotope data and field observations—that samples from sampling sites with low RSDs (e.g., Panther Rocks, Duncan Knob, Miller Rock) have lost mass by steady granular disintegration or the peeling of thin sheets rather than by shedding thick slabs. Sites with high RSDs (e.g., Buzzards Rock, Turtle Rocks, Rock Ridge) most likely include a sample from a surface exposed after block failure or from one that is likely to experience a loss of mass by block failure in the near future.

Semivariogram results show that our measured erosion rates are spatially autocorrelated at two distances: 68 km and 196 km (Fig. 6). The 68 km decorrelation distance is large enough for erosion rates from each sampling site to be correlated to those from the next-closest sampling sites. Similar to the observed average deviation, the 68 km decorrelation distance reflects observations showing outcrops eroding more similarly to other nearby outcrops than to those at greater distances. The second decorrelation distance suggests that erosion rates are also correlated at a distance of 196 km, though the interpretation is less clear. At 196 km, observations suggest that all measured erosion rates separated by this distance are more correlated to each other than erosion rates at greater separation distances. This distance likely reflects a correlation between erosion rates of outcrops in a physiographic province from one drainage basin to those in the same physiographic province in the other drainage basin (Fig. 6), an observation consistent with the results of Student's t-tests showing similarity among the means of these rates (Fig. 5F). Correlations between erosion

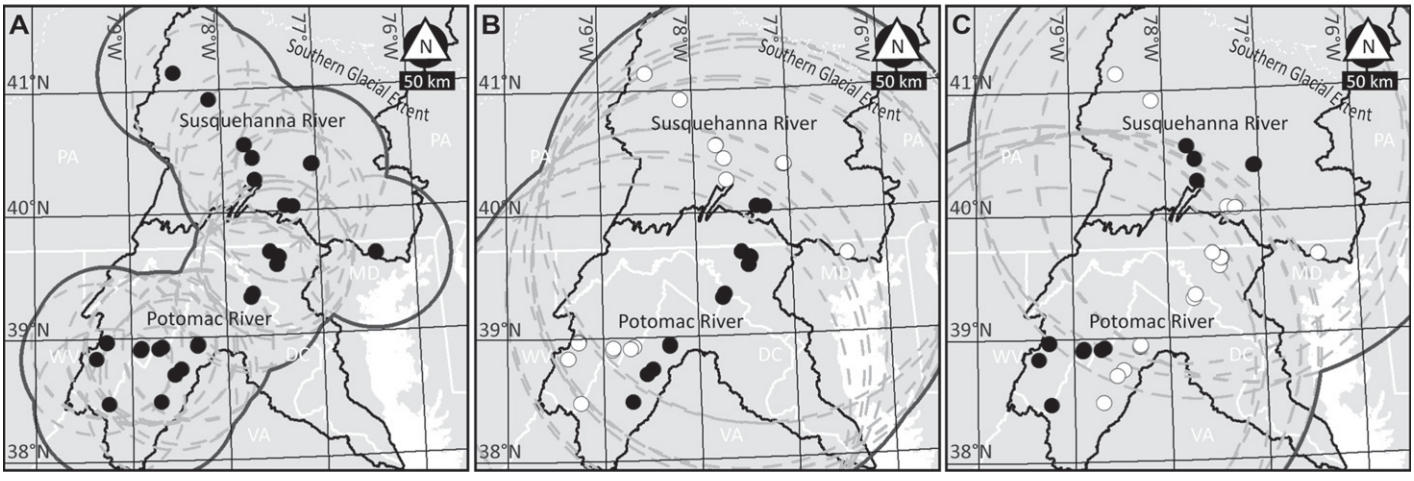

Figure 6. Outcrop erosion rates are spatially autocorrelated at two distances in our study area. (A) Map of the study area illustrating the 68 km decorrelation distance determined from semivariogram analyses (Fig. 4). Light-gray, dashed circles represent a 68 km radius around each sampled outcrop, while the darker-gray line marks the perimeter of the overall area of spatial autocorrelation. The 65 km distance represents the distance from one sampling site to the next. (B) Map of the study area illustrating the 196 km decorrelation distance between outcrops from the Blue Ridge Province. (C) Map of the study area illustrating the 196 km decorrelation distance between outcrops from the Valley and Ridge Province. The 196 km distance indicates that erosion rates from outcrops from one physiographic province in one basin are spatially autocorrelated to those from the same physiographic province of the other basin.

rates in the same physiographic province, no matter the distance between them, may be due to underlying structural, lithological, or mechanical properties of the rock within a province such as the specific mineralogy, type of cementation, dip of strata, joint and fracture spacing in the outcrop, or rock hardness.

Comparing Erosion Rates to Other Studies

Inferred outcrop erosion rates from three previous studies in the central Appalachian Mountains (Duxbury, 2009; Hancock and Kirwan, 2007; Reuter, 2005) are consistent with our conclusion that the landscape is slowly changing (Fig. 7). An ANOVA reveals no significant difference among the means of sample populations from these studies ($p = 0.44$), and results from a Tukey-Kramer HSD analysis indicate equality between the means of each sample population ($p > 0.42$; Fig. 7). Average bedrock outcrop erosion rates in the central Appalachian Mountains (9 m m.y.$^{-1}$) are also consistent with bedrock outcrop erosion rates in quiescent tectonic settings around the world ($n = 299$) inferred from cosmogenic ^{10}Be (12 m m.y.$^{-1}$; $p = 0.18$; Fig. 8; Portenga and Bierman, 2011).

Basin-averaged erosion rates from 178 central Appalachian watersheds with basin-average slopes ranging from ~1° to 24° result in a mean watershed erosion rate of 15 m.y.$^{-1}$, which is higher than the average erosion rate estimated from exposed bedrock outcrops (9 m m.y.$^{-1}$) in the central Appalachian Mountains (Duxbury, 2009; Reuter, 2005; Trodick, 2011; Fig. 9). Within the Potomac River Basin, outcrop erosion rates (9.6 m m.y.$^{-1}$; $n = 45$) are just slightly less than those of drainage basins (10 m m.y.$^{-1}$; $n = 99$; $p = 0.01$) determined from multiple other studies (e.g., Duxbury, 2009; Trodick, 2011). Because our focus is identifying erosion patterns within the Potomac River Basin, only basins draining westward from Shenandoah National Park into the Potomac River Basin were used for this statistical comparison (Duxbury, 2009). In contrast, in the Susquehanna River Basin, the average drainage basin erosion rate (20 m m.y.$^{-1}$; $n = 79$; Reuter, 2005) is more than twice that of bedrock outcrops (8 m m.y.$^{-1}$; $n = 26$; $p < 0.01$; Fig. 9).

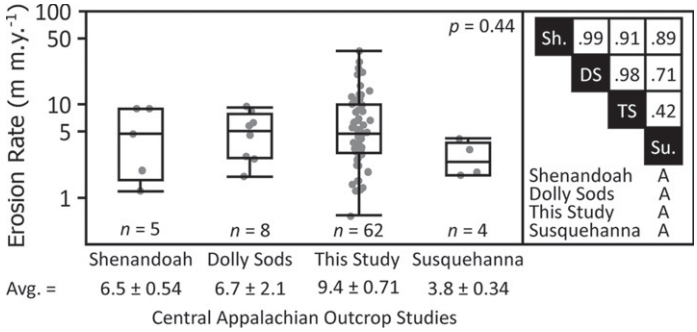

Figure 7. Box and whisker plots of outcrop erosion rates used in analysis of variance (ANOVA) comparing average erosion rates from bedrock outcrops in the central Appalachian region, including those from Shenandoah National Park (Duxbury, 2009), Dolly Sods in West Virginia (Hancock and Kirwan, 2007), and sites in the Susquehanna River Basin (Reuter, 2005). Outcrop locations for all studies can be found in Figure 1. Results and *p* values of a Tukey-Kramer honestly significant difference (HSD) analyses are shown in the stair-step chart. The ends of the whiskers mark the range of erosion rates in each category, while the top, middle, and bottom of each box mark the 75th, 50th, and 25th percentiles, respectively. Gray dots represent individual erosion rate samples.

At face value, the disparity between basin-averaged and outcrop erosion rates suggests that relief is increasing in both drainage basins, though at a much greater rate in the Susquehanna River Basin (Fig. 9). There are, however, other plausible explanations for our observations. Periglacial activity may have accelerated mass loss from basin slopes, introducing once-shielded and less-dosed material into the region's streams while outcrops were less affected. Another possibility is that basin-averaged erosion rates may reflect the influence of

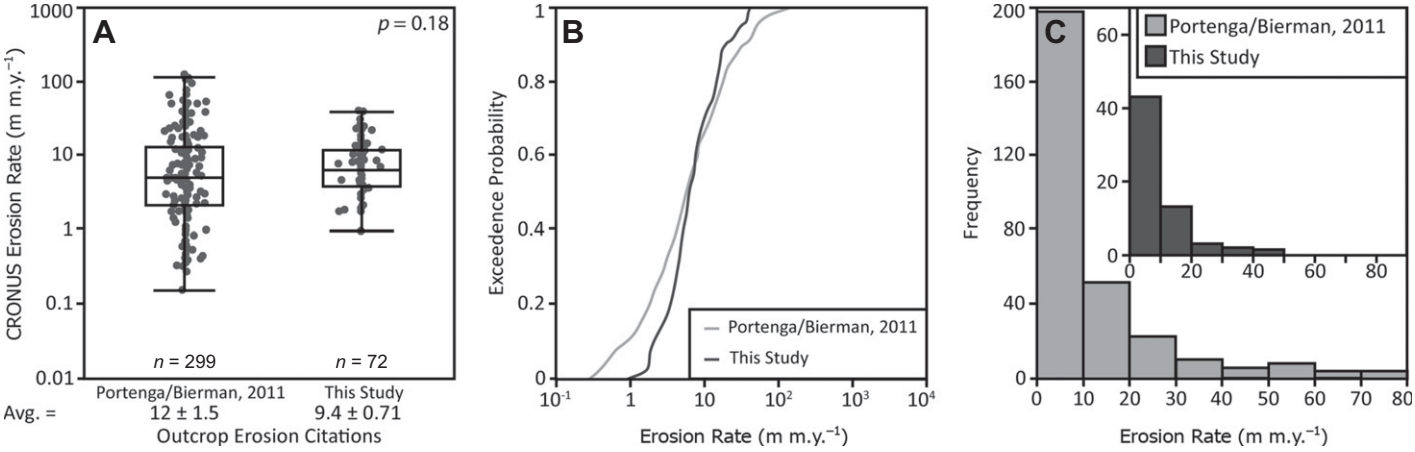

Figure 8. (A) Data used in a Student's *t*-test comparing the means of outcrop erosion rates in quiescent tectonic settings from around the world ($n = 299$; Portenga and Bierman, 2011) and in the central Appalachian Mountains. (B) Exceedance probability of global ^{10}Be erosion rates (light-gray line) shows a wider distribution than samples from this study (dark-gray line). (C) Histograms of cosmogenic ^{10}Be erosion rates around the world (light-gray bars) and this study (inset dark-gray bars), both showing a skewed distribution toward low erosion rates.

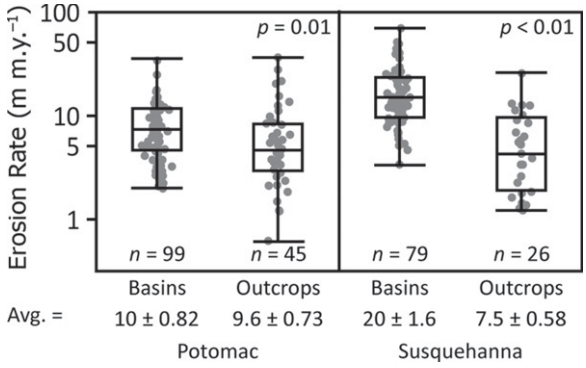

Figure 9. Data used in a Student's *t*-test analysis comparing the means of basin-averaged and outcrop erosion rates in the Potomac and Susquehanna River Basins. Both analyses show basin-averaged erosion rates in each river system to be significantly higher than outcrop erosion rates. Samples come from this study and numerous others (Duxbury, 2009; Reuter, 2005; Trodick, 2011). Only westward-draining basins from the Duxbury (2009) study in Shenandoah National Park were used for this analysis; eastward-draining basins are not part of the Potomac River drainage system.

deep-seated mass movements, perhaps triggered by torrential hurricane rains, delivering less-dosed material to the channels (Adams and Spotila, 2005; Eaton et al., 2003; Mills, 1981; Niemi et al., 2005; Tucker and Bras, 2000). Conversely, basin-averaged erosion rates may reflect transients in landscape behavior such as rapid downcutting following stream-capture events and effective base-level fall, ideas initially envisioned by Davis (1899). Examples of transient landscape conditions could be associated with the southwest migration of the continental divide in the central Appalachian Mountains past the Blue Ridge and into the Valley and Ridge (e.g., Clark, 1989; Erickson and Harbor, 1998; Harbor et al., 2005; Naeser et al., 2001; Prince et al., 2010), although such transients may not be apparent from our outcrop erosion data set alone.

Implications for Large-Scale Landscape Evolution

Methods integrating over many millions of years and larger areas tend to result in higher erosion rates than those estimated for bedrock outcrops. For example, rates of erosion inferred from ^{10}Be in bedrock outcrops are two to three times lower than denudation rates determined from sediment fluxes to offshore basins (i.e., Pazzaglia and Brandon, 1996; Sevon, 1989), from (U-Th)/He dating (i.e., Reed et al., 2005; Spotila et al., 2004), and from fission-track thermochronologies (i.e., Blackmer et al., 1994; Boettcher and Milliken, 1994; C.W. Naeser et al., 2001, 2005; N.D. Naeser et al., 2004; Reed et al., 2005; Spotila et al., 2004) integrating denudation since ca. 300 Ma to the present (~21 m m.y.$^{-1}$; Fig. 10). This implies that over millennial time scales, stable ridgelines control, at least in part, the evolution of Appalachian landscapes. Perhaps, denudation rates on longer time scales are higher because they incorporate erosion during multiple glaciations and reflect higher levels of isostatic uplift.

The similarly low erosion and denudation rates from thermochronologic, basin-averaged cosmogenic, and sediment flux studies confirm a history of slow landscape lowering in the central Appalachian Mountains since post-Alleghenian rifting events and most likely reflect isostatically driven rebound responding to mass loss by erosion. Such similarity between erosion rates on cosmogenic and thermochronologic time scales is not uncommon. Similar observations have been made in Namibia (Cockburn et al., 2000), the California Sierra Nevada (Granger et al., 2001), and Sri Lanka (von Blanckenburg et al., 2004). The offset between basin-scale and ridgeline outcrop cosmogenic erosion rate estimates is consistent with increasing relief over the later Pleistocene. Conversely, it could be an artifact of the way in which ridgeline outcrops erode: While erosion from above is slow, erosion from the margins is more rapid, eventually destroying ridgelines from the side. Such a scenario suggests that stable ridgelines themselves are transient landscape features and would resolve the disparity between erosion rate estimates at different time and spatial scales.

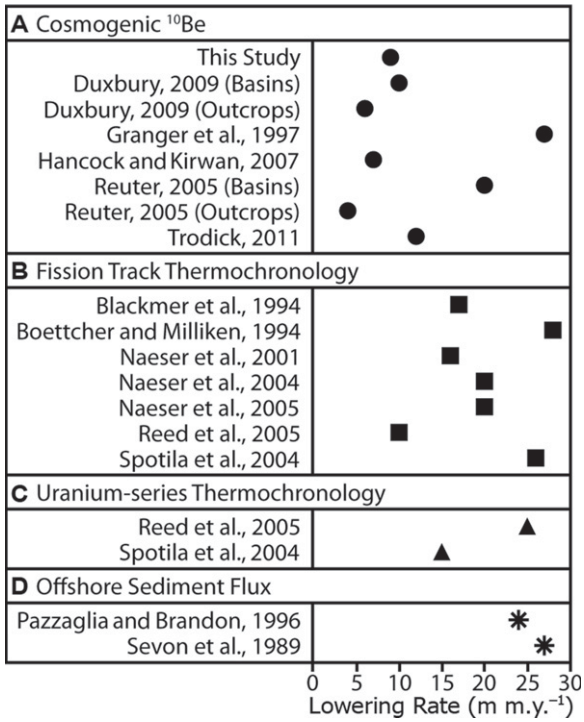

Figure 10. Average erosion and denudation rates for the study area determined by multiple methods. (A) Concentrations of ^{10}Be in exposed bedrock outcrops and fluvial sediment (circles). (B) Fission-track thermochronology (squares). (C) (U-Th)/He thermochronology (triangles). (D) Sediment flux to offshore depositional basins (stars).

CONCLUSIONS

The central Appalachian Mountains include slowly changing landscapes in the Potomac and Susquehanna River Basins. The highest ridgelines in the area are eroding slowly (on average 9 m m.y.$^{-1}$) and have been for at least tens to hundreds of thousands of years. Though there is spatial variability in bedrock outcrop erosion rates along ridgelines, the median erosion rate (6 m m.y.$^{-1}$) shows that mass in this region is not quickly removed from exposed outcrops.

Outcrop erosion rates vary. Single environmental parameters, either alone or considered together, explain only a small part (22%) of the erosion rate variability we measured in the central Appalachians; much of the unexplained variability is likely related to specific properties of each rock outcrop, including joint spacing,

rock strength, mineralogy, and porosity. The factors, whether environmental or physical, that control erosion rates of exposed rock remain uncertain.

Average erosion rates from cosmogenic ^{10}Be in bedrock outcrops on main ridgelines (this study and others) are consistent with data from other methods integrating over longer time windows and indicate that the central Appalachian Mountains have been wearing down at rates no more than a few tens of meters per million years since post-Triassic rifting events. The disparity between outcrop- and basin-scale rates of erosion is consistent with an increase in relief over the cosmogenic time scale (tens to hundreds of thousands of years) or a process by which stable ridgelines are eventually destroyed by erosion from their perimeters.

ACKNOWLEDGMENTS

We thank R. Harriett (Harpers Ferry National Historical Park), B. Loncoski (Catoctin Mountain Park), B. Norden (Maryland Department of Natural Resources), T. Collins (George Washington National Forest), L. Tracey (Monongahela National Forest), S. Summers (West Virginia Division of Natural Resources), and G. Blackmer (Pennsylvania Department of Conservation and Natural Resources) for assistance in obtaining permits and C. Trodick Jr. for his help in collecting samples. We also thank Gregory Hancock and James Spotila for their thoughtful and constructive comments and guidance throughout the review process. This work was supported by National Science Foundation grant EAR-310208 and U.S. Geological Survey grant 08ERSA0582 and was performed in part under the auspices of the U.S. Department of Energy at Lawrence Livermore National Laboratory under contract DE-AC52-07NA27344.

REFERENCES CITED

Adams, R.K., and Spotila, J.A., 2005, The form and function of headwater streams based on field and modeling investigations in the southern Appalachian Mountains: Earth Surface Processes and Landforms, v. 30, p. 1521–1546, doi:10.1002/esp.1211.

Balco, G., Stone, J.O., Lifton, N.A., and Dunai, T.J., 2008, A complete and easily accessible means of calculating surface exposure ages or erosion rates from ^{10}Be and ^{26}Al measurements: Quaternary Geochronology, v. 3, p. 174–195, doi:10.1016/j.quageo.2007.12.001.

Bierman, P., and Caffee, M., 2002, Cosmogenic exposure and erosion history of Australian bedrock landforms: Geological Society of America Bulletin, v. 114, no. 7, p. 787–803, doi:10.1130/0016-7606(2002)114<0787:CEAEHO>2.0.CO;2.

Bierman, P., and Steig, E.J., 1996, Estimating rates of denudation using cosmogenic isotope abundances in sediment: Earth Surface Processes and Landforms, v. 21, p. 125–139, doi:10.1002/(SICI)1096-9837(199602)21:2<125::AID-ESP511>3.0.CO;2-8.

Blackmer, G.C., Omar, G.I., and Gold, D.P., 1994, Post-Alleghanian unroofing history of the Appalachian Basin, Pennsylvania, from apatite fission track analysis and thermal models: Tectonics, v. 13, p. 1259–1276, doi:10.1029/94TC01507.

Boettcher, S.S., and Milliken, K.L., 1994, Mesozoic-Cenozoic unroofing of the southern Appalachian Basin: Apatite fission track evidence from Middle Pennsylvanian sandstones: The Journal of Geology, v. 102, p. 655–668, doi:10.1086/629710.

Braun, D.D., 1989, Glacial and periglacial erosion of the Appalachians: Geomorphology, v. 2, p. 233–256, doi:10.1016/0169-555X(89)90014-7.

Braun, D.D., 1993, Evidence for periglacial mobilization of the Piedmont land surface in northern Maryland, *in* Ford, D., and McCann, B., Third International Geomorphology Conference: Hamilton, Canada, McMaster University, Programme with Abstracts.

Brown, E.T., Stallard, R.F., Larsen, M.C., Raisbeck, G.M., and Yiou, F., 1995, Denudation rates determined from the accumulation of in situ–produced ^{10}Be in the Luquillo Experimental Forest, Puerto Rico: Earth and Planetary Science Letters, v. 129, p. 193–202, doi:10.1016/0012-821X(94)00249-X.

Chmeleff, J., von Blanckenburg, F., Kossert, K., and Jakob, D., 2010, Determination of the ^{10}Be half-life by multicollector ICP-MS and liquid scintillation counting: Nuclear Instruments & Methods in Physics Research, Section B, Beam Interactions with Materials and Atoms, v. 268, no. 2, p. 192–199, doi:10.1016/j.nimb.2009.09.012.

Clark, G.M., 1989, Central and southern Appalachian water and wind gap origins: Review and new data: Geomorphology, v. 2, p. 209–232, doi:10.1016/0169-555X(89)90013-5.

Cockburn, H.A.P., Brown, R.W., Summerfield, M.A., and Seidl, M.A., 2000, Quantifying passive margin denudation and landscape development using a combined fission-track thermochronology and cosmogenic isotope analysis approach: Earth and Planetary Science Letters, v. 179, p. 429–435, doi:10.1016/S0012-821X(00)00144-8.

Davis, W.M., 1899, The geographical cycle: The Geographical Journal, v. 14, no. 5, p. 481–504, doi:10.2307/1774538.

Delunel, R., Beek, P.A.d., Carcaillet, J., Bourlès, D.L., and Valla, P.G., 2010, Frost-cracking control on catchment denudation rates: Insights from in situ produced ^{10}Be concentrations in stream sediments (Ecrins-Pelvoux massif, French western Alps): Earth and Planetary Science Letters, v. 293, p. 72–83, doi:10.1016/j.epsl.2010.02.020.

Dunne, J., Elmore, D., and Muzikar, P., 1999, Scaling factors for the rates of production of cosmogenic nuclides for geometric shielding and attenuation at depth on sloped surfaces: Geomorphology, v. 27, p. 3–11, doi:10.1016/S0169-555X(98)00086-5.

Duxbury, J., 2009, Erosion Rates In and Around Shenandoah National Park, VA, Determined Using Analysis of Cosmogenic ^{10}Be [M.S. thesis]: Burlington, Vermont, University of Vermont, 134 p.

Eaton, L.S., Morgan, B.A., Kochel, R.C., and Howard, A.D., 2003, Role of debris flows in long-term landscape denudation in the central Appalachians of Virginia: Geology, v. 31, no. 4, p. 339–342, doi:10.1130/0091-7613(2003)031<0339:RODFIL>2.0.CO;2.

Erickson, P.A., and Harbor, D.J., 1998, Bringing down Floyd: Incision by the James River in the Valley and Ridge of Virginia: Geological Society of America Abstracts with Programs, v. 30, no. 7, p. 142.

Granger, D.E., Kirchner, J.W., and Finkel, R., 1996, Spatially averaged long-term erosion rates measured from in situ–produced cosmogenic nuclides in alluvial sediment: The Journal of Geology, v. 104, p. 249–257, doi:10.1086/629823.

Granger, D.E., Kirchner, J.W., and Finkel, R.C., 1997, Quaternary downcutting rate of the New River, Virginia, measured from differential decay of cosmogenic ^{26}Al and ^{10}Be in cave-deposited alluvium: Geology, v. 25, no. 2, p. 107–110, doi:10.1130/0091-7613(1997)025<0107:QDROTN>2.3.CO;2.

Granger, D.E., Riebe, C.S., Kirchner, J.W., and Finkel, R.C., 2001, Modulation of erosion on steep granitic slopes by boulder armoring, as revealed by cosmogenic ^{26}Al and ^{10}Be: Earth and Planetary Science Letters, v. 186, p. 269–281, doi:10.1016/S0012-821X(01)00236-9.

Gunnell, Y., and Harbor, D.J., 2010, Butte detachment: How pre-rift geological structure and drainage integration drive escarpment evolution at rifted continental margins: Earth Surface Processes and Landforms, v. 35, no. 12, p. 1373–1385, doi:10.1002/esp.1973.

Hack, J.T., 1960, Interpretation of erosional topography in humid temperate regions: American Journal of Science, v. 258-A, p. 80–97.

Hales, T.C., and Roering, J.J., 2007, Climatic controls on frost cracking and implications for the evolution of bedrock landscapes: Journal of Geophysical Research, v. 112, F02033, doi:10.1029/2006JF000616.

Hancock, G., and Kirwan, M., 2007, Summit erosion rates deduced from ^{10}Be: Implications for relief production in the central Appalachians: Geology, v. 35, no. 1, p. 89–92, doi:10.1130/G23147A.1.

Harbor, D., Bacastow, A., Heath, A., and Rogers, J., 2005, Capturing variable knickpoint retreat in the Central Appalachians, USA: Geografia Fisica e Dinamica Quaternaria, v. 28, no. 1, p. 23–36.

Heimsath, A.M., Dietrich, W.E., Nishiizumi, K., and Finkel, R.C., 1997, The soil production function and landscape equilibrium: Nature, v. 388, p. 358–361, doi:10.1038/41056.

Heimsath, A.M., Dietrich, W.E., Nishiizumi, K., and Finkel, R.C., 1999, Cosmogenic nuclides, topography, and the spatial variation of soil depth: Geomorphology, v. 27, p. 151–172, doi:10.1016/S0169-555X(98)00095-6.

Hijmans, R.J., Cameron, S.E., Parra, J.L., Jones, P.G., and Jarvis, A., 2005, Very high resolution interpolated climate surfaces for global land areas: International Journal of Climatology, v. 25, p. 1965–1978, doi:10.1002/joc.1276.

Issaks, E.H., and Srivastava, R.M., 1989, An Introduction to Applied Geostatistics: New York, Oxford University Press, 592 p.

Journel, A.G., and Huijbregts, C., 1978, Mining Geostatistics: New York, Academic Press, 600 p.

Kohl, C.P., and Nishiizumi, K., 1992, Chemical isolation of quartz for measurement of in-situ–produced cosmogenic nuclides: Geochimica et Cosmochimica Acta, v. 56, p. 3583–3587, doi:10.1016/0016-7037(92)90401-4.

Korschinek, G., Bergmaier, A., Faestermann, T., Gerstmann, U.C., Knie, K., Rugel, G., Wallner, A., Dillmann, I., Dollinger, G., Gostomski, C.L.v., Kossert, K., Maiti, M., Poutivtsev, M., and Remmert, A., 2010, A new value for the half-life of ^{10}Be by heavy-ion elastic recoil detection and liquid scintillation counting: Nuclear Instruments & Methods in Physics Research, Section B, Beam Interactions with Materials and Atoms, v. 268, p. 187–191, doi:10.1016/j.nimb.2009.09.020.

Lal, D., 1991, Cosmic ray labeling of erosion surfaces: In situ nuclide production rates and erosion models: Earth and Planetary Science Letters, v. 104, p. 424–439, doi:10.1016/0012-821X(91)90220-C.

Mills, H.H., 1981, Boulder deposits and the retreat of mountain slopes, or, "gully gravure" revisited: The Journal of Geology, v. 89, p. 649–660, doi:10.1086/628628.

Montgomery, D.R., and Brandon, M.T., 2002, Topographic controls on erosion rates in tectonically active mountain ranges: Earth and Planetary Science Letters, v. 201, p. 481–489, doi:10.1016/S0012-821X(02)00725-2.

Naeser, C.W., Naeser, N.D., Kunk, M.J., Morgan, B.A., III, Schultz, A.P., Southworth, C.S., and Weems, R.E., 2001, Paleozoic through Cenozoic uplift, erosion, stream capture, and deposition history in the Valley and Ridge, Blue Ridge, Piedmont, and Coastal Plain province of Tennessee, North Carolina, Virginia, Maryland, and District of Columbia: Geological Society of America Abstracts with Programs, v. 33, no. 6, p. 312.

Naeser, C.W., Naeser, N.D., and Southworth, S., 2005, Tracking across the southern Appalachians, *in* Hatcher, R.D., and Merschat, A.J., eds., Blue Ridge Geology Geotraverse East of the Great Smoky Mountains National Park, Western North Carolina: North Carolina Geological Survey, Carolina Geological Society Annual Field Trip Guidebook, p. 67–72.

Naeser, N.D., Naeser, C.W., Southworth, C.S., Morgan, B.A., and Schultz, A.P., 2004, Paleozoic to Recent tectonic and denudation history of rocks in the Blue Ridge Province, central and southern Appalachians; evidence from fission-track thermochronology: Geological Society of America Abstracts with Programs, v. 36, no. 2, p. 114.

Niemi, N.A., Oskin, M., Burbank, D.W., Heimsath, A.M., and Gabet, E.J., 2005, Effects of bedrock landslides on cosmogenically determined erosion rates: Earth and Planetary Science Letters, v. 237, p. 480–498, doi:10.1016/j.epsl.2005.07.009.

Nishiizumi, K., Lal, D., Klein, J., Middleton, R., and Arnold, J.R., 1986, Production of ^{10}Be and ^{26}Al by cosmic

rays in terrestrial quartz in situ and implications for erosion rates: Nature, v. 319, p. 134–136, doi:10.1038/319134a0.

Nishiizumi, K., Imamura, M., Caffee, M.W., Southon, J.R., Finkel, R.C., and McAninch, J., 2007, Absolute calibration of ^{10}Be AMS standards: Nuclear Instruments & Methods in Physics Research, Section B, Beam Interactions with Materials and Atoms, v. 258, p. 12,143–12,157, doi:10.1016/j.nimb.2007.01.297.

Pazzaglia, F.J., and Brandon, M.T., 1996, Macrogeomorphic evolution of the post-Triassic Appalachian Mountains determined by deconvolution of the offshore basin sedimentary record: Basin Research, v. 8, p. 255–278, doi:10.1046/j.1365-2117.1996.00274.x.

Pazzaglia, F.J., and Gardner, T.W., 1994, Late Cenozoic flexural deformation of the middle U.S. Atlantic passive margin: Journal of Geophysical Research, v. 99, p. 143–157, doi:10.1029/93JB03130.

Peel, M.C., Finlayson, B.L., and McMahon, T.A., 2007, Updated world map of the Köppen-Geiger climate classification: Hydrology and Earth System Sciences, v. 11, p. 1633–1644, doi:10.5194/hess-11-1633-2007.

Poag, C.W., and Sevon, W.D., 1989, A record of Appalachian denudation in postrift Mesozoic and Cenozoic sedimentary deposits of the U.S. middle Atlantic continental margin: Geomorphology, v. 2, p. 119–157, doi:10.1016/0169-555X(89)90009-3.

Portenga, E.W., and Bierman, P.R., 2011, Understanding Earth's eroding surface with ^{10}Be: GSA Today, v. 21, no. 8, p. 4–10, doi:10.1130/G111A.1.

Prince, P.S., Spotila, J.A., and Henika, W.S., 2010, New physical evidence of the role of stream capture in active retreat of the Blue Ridge Escarpment, southern Appalachians: Geomorphology, v. 123, p. 305–319, doi:10.1016/j.geomorph.2010.07.023.

Reed, J.S., Spotila, J.A., Eriksson, K.A., and Bodnar, R.J., 2005, Burial and exhumation history of Pennsylvanian strata, central Appalachian Basin: An integrated study: Basin Research, v. 17, p. 259–268, doi:10.1111/j.1365-2117.2005.00265.x.

Reusser, L., Bierman, P., Pavich, M., Larsen, J., and Finkel, R., 2006, An episode of rapid bedrock channel incision during the last glacial cycle, measured with ^{10}Be: American Journal of Science, v. 306, p. 69–102, doi:10.2475/ajs.306.2.69.

Reuter, J., 2005, Erosion Rates and Patterns Inferred from Cosmogenic ^{10}Be in the Susquehanna River Basin [M.S. thesis]: Burlington, Vermont, University of Vermont, 172 p.

Roden, M.K., 1991, Apatite fission-track thermochronology of the southern Appalachian Basin: Maryland, West Virginia, and Virginia: The Journal of Geology, v. 99, p. 41–53, doi:10.1086/629472.

Saunders, I., and Young, A., 1983, Rates of surface processes on slopes, slope retreat, and denudation: Earth Surface Processes and Landforms, v. 8, p. 473–501, doi:10.1002/esp.3290080508.

Sevon, W.D., 1989, Erosion in the Juniata River drainage basin, Pennsylvania: Geomorphology, v. 2, p. 303–318, doi:10.1016/0169-555X(89)90017-2.

Small, E.E., Anderson, R.S., Repka, J.L., and Finkel, R., 1997, Erosion rates of alpine bedrock summit surfaces deduced from in situ ^{10}Be and ^{26}Al: Earth and Planetary Science Letters, v. 150, p. 413–425, doi:10.1016/S0012-821X(97)00092-7.

Spotila, J.A., Bank, G.C., Reiners, P.W., Naeser, C.W., Naeser, N.D., and Henika, B.S., 2004, Origin of the Blue Ridge Escarpment along the passive margin of eastern North America: Basin Research, v. 16, p. 41–63, doi:10.1111/j.1365-2117.2003.00219.x.

Stone, J.O., 2000, Air pressure and cosmogenic isotope production: Journal of Geophysical Research, v. 105, no. B10, p. 23,753–23,759, doi:10.1029/2000JB900181.

Trodick, C.D., 2011, In Situ and Meteoric ^{10}Be Concentrations of Fluvial Sediment Collected from the Potomac River Basin [M.S. thesis]: Burlington, Vermont, University of Vermont, 213 p.

Tucker, G.E., and Bras, R.L., 2000, A stochastic approach to modeling the role of rainfall variability in drainage basin evolution: Water Resources Research, v. 36, no. 7, p. 1953–1964, doi:10.1029/2000WR900065.

von Blanckenburg, F., Hewawasam, T., and Kubik, P.W., 2004, Cosmogenic nuclide evidence for low weathering and denudation in the wet, tropical highlands of Sri Lanka: Journal of Geophysical Research, v. 109, F03008, doi:10.1029/2003JF000049.

Wakasa, S., Matsuzaki, H., Tanaka, Y., and Matsukura, Y., 2006, Estimation of episodic exfoliation rates of rock sheets on a granite dome in Korea from cosmogenic nuclide analysis: Earth Surface Processes and Landforms, v. 31, p. 1246–1256, doi:10.1002/esp.1328.

Ward, D.J., Spotila, J.A., Hancock, G.S., and Galbraith, J.M., 2005, New constraints on the late Cenozoic incision history of the New River, Virginia: Geomorphology, v. 72, p. 54–72, doi:10.1016/j.geomorph.2005.05.002.

Science Editor: Nancy Riggs
Associate Editor: Benjamin J.C. Laabs

Manuscript Received 27 May 2011
Revised Manuscript Received 28 May 2012
Manuscript Accepted 2 July 2012

Printed in the USA